25th ABCM International Congress of Mechanical Engineering
October 20-25, 2019, Uberlândia, MG, Brazil

COB-2019-1287
SCALING OF THE FAR FIELD PRESSURE OF IN-FLIGHT JETS SIMULATED WITH AN OPEN JET WIND TUNNEL

Anderson R. Proença
Jack L. T. Lawrence
Rod H. Self
Institute of Sound and Vibration Research, University of Southampton, Southampton, UK
a.proenca@soton.ac.uk, j.lawrence@soton.ac.uk, rhs@isvr.soton.ac.uk

Abstract. *This paper presents an experimental investigation into the far pressure field of in-flight jets. The aim of this work is to evaluate the representativeness of finite flight-stream in comparison to the full-scale problem, that is, a jet exhausted from an aircraft engine during the take-off phase. A second objective is to investigate the scaling of the pressure field with both jet and flight velocities. An open jet wind tunnel has been used to simulate forward flight effects on jet mixing noise. Jet far field pressure measurements have been acquired at ten observer polar angles. Analysis of the results suggests that the jet mixing noise scale well with the eighth power of the difference between the jet velocity and flight-stream speed. This is expected from the dimensional analysis of the governing equations (Lighthill's acoustic analogy). The far field pressure scaling law is also in agreement with aerodynamic measurements performed in the jet flow. Finally, investigation of the overall sound pressure levels shows that the stretching of the jet and changes in eddy convection velocity due to a forward flight flow affects the directivity of the sound waves in the jet far field. It is hoped that the experimental evidence presented in this paper will improve understanding of the advantages and limitations of using small-scale open jet wind tunnels to survey forward flight effects on jet noise.*

Keywords: *jet noise, forward flight effects, wind tunnel, aeroacoustics, jet rig*

1. INTRODUCTION

In large, developed cities, aircraft are one of the main sources of environmental noise. The number of average daily flights are set to increase substantially in the years to come. Urban areas around airports are also growing over time, expanding the community under an aircraft flightpath. During take-off, the air jet exhausted by the engine of a modern aircraft still is one of the dominant noise sources. Therefore, predicting and mitigating the jet noise component is essential to achieve acceptable levels of noise produced by future aircraft.

The noise produced by jets discharged into quiescent media, or static jets, have been extensively studied since the early 1950s. Lighthill's Acoustic Analogy, an exact rearrangement of the Navier-Stokes equations used to calculate the sound generated by aerodynamic sound, was developed to understand how a turbulent jet flow produces noise (Lighthill, 1952). Other acoustic analogies as well as instability models have been developed to improve understanding of the jet noise source, but the fundamental physics involved in this problem seems far from been accepted as commonplace. The forward flight effects on jet noise, for example, is an important element of the engine noise problem and it is not trivial. The turbulent jet exhausted at a given velocity by a moving engine is considerably different from its static jet counterpart both in terms of aerodynamics and acoustics.

Several experiments on in-flight jets were carried out in the 1970s. These tests were performed mainly in two types of flight-jet rigs. In the first type of flight-jet rig, the jet nozzle is surrounded by a coaxial, open jet wind tunnel. The microphones are located outside the flow produced by this wind tunnel, or 'flight' flow. Examples of these facilities were used in the UK, at the NGTE Pyestock (Cocking and Bryce, 1975), in the USA at NASA (Plumblee, 1976; Tanna and Morris, 1977) and Pratt & Whitney (Larson *et al.*, 1978). Another arrangement would consist of actually moving the jet nozzle, or engine, at the desirable speed, as in the full-scale application. Test data of this kind were performed by the French company SNECMA using the tracked air cushion vehicle Aérotrain (Drevet *et al.*, 1977). The advantages and disadvantages of each method were discussed by Morris and Viswanathan (Camussi, 2013).

Fundamental questions on this subject are still open. Are small-scale open jet wind tunnel rigs capable of representing the forward flight effects seen in a moving engine? Why does the scaling of far field pressure with jet and flight velocities vary between different flight-jet facilities? Does the flight flow changes the convection of the jet mixing noise sources? The list goes on. In the present work, the far field of in-flight jets were investigated experimentally. An open jet wind tunnel was used to simulate forward flight effects around a core jet. Both the core jet velocity and the flight velocity

were varied systematically. Results are analysed to complement a recent investigation into the jet turbulent flow field of in-flight jets (Proenca *et al.*, 2019). A direct link between aerodynamic and acoustics results is provided, especially the effects of jet stretching in the pressure far field. An example of the jet stretching with flight velocity is displayed in Fig. 1.

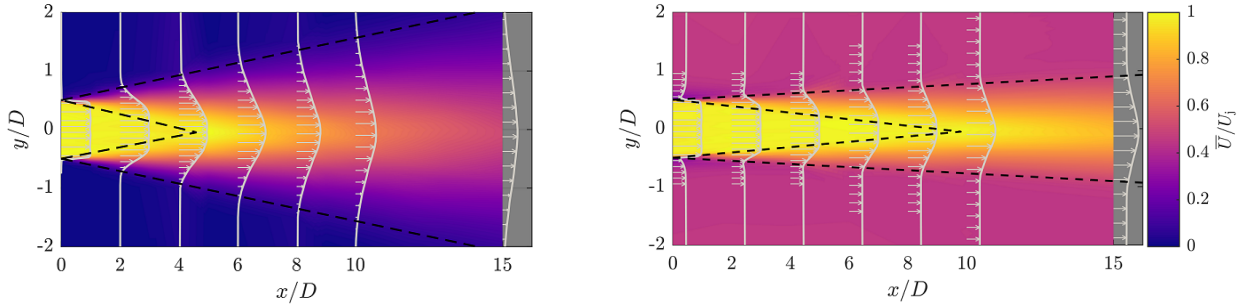

(a) Static jet, $M_f = 0$ (b) In-flight jet, $M_f = 0.3$

Figure 1. Mean velocity profiles showing the jet stretching with flight velocity. The potential core and edge of the shear layer are illustrated by dashed lines (adapted from Proenca (2018))

The paper is structured as follows. In the next section, the experimental methodology is provided. The facility, instruments used, data acquisition system and data post-processing are discussed. In Section 3, results are presented and discussed. Firstly, general results are shown. Then, scaling of the sound pressure levels and overall sound pressure levels with jet and flight velocities are analysed. Finally, the main conclusions are discussed in Section 4.

2. EXPERIMENTAL METHODOLOGY

2.1 Experimental facility

The experiments were performed in the Doak Laboratory, at the University of Southampton, UK. The Doak Lab. is an anechoic chamber down to 300 Hz. A flight-jet rig was mounted in the chamber. Figure 2(a) displays the flight and the core jet nozzles. Both the flight and the jet flows produce cold, round, subsonic jets. The flight rig can reach a Mach number just above 0.3 and the jet rig reaches sonic speeds. A microphone fly over array was installed above the jets to measure the pressure field. A schematic showing the definition of the observer polar angles is displayed in Figure 2(b).

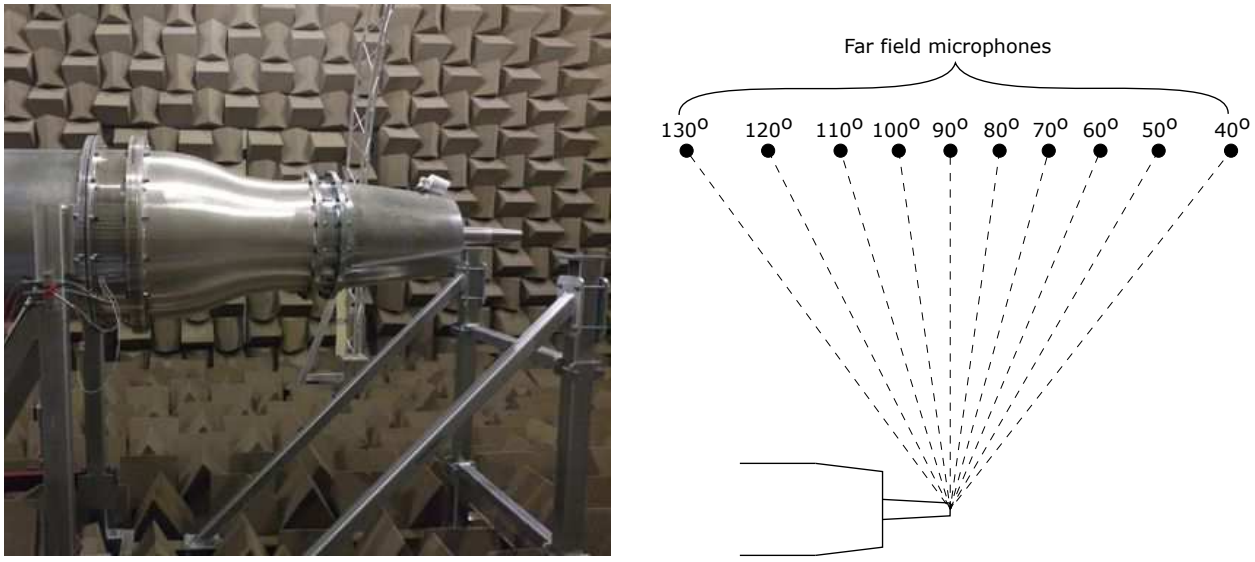

(a) Flight-jet rig (b) Fly over far field array

Figure 2. Experimental facility: (a) The flight-jet rig in the Doak Laboratory. (b) Schematics of the fly-over array and polar angles studied in this work

The flight and jet round nozzles have exit diameters of 0.3 m and 0.04 m, respectively. More information about the anechoic chamber and the flight-jet rig can be found in Proenca et al. (Proenca, 2018; Proenca *et al.*, 2019).

2.2 Instrumentation

Pressure and temperature probes were installed in the chamber and in the rig to set the nominal velocity of both the core jet and the flight flow. The relative humidity inside the chamber was also measured to apply correction for the atmospheric attenuation on the sound propagation. Real time ambient and flow properties data were used with isentropic equations to set and maintain the nominal velocities. Eight core jet velocities, ranging from $M_\mathrm{j} = 0.2$ to 0.9 at 0.1 intervals, were set. Flight velocities analysed vary from $M_\mathrm{f} = 0$ (the static case) to 0.3 at 0.05 intervals.

One-quarter inch GRAS Type 40BF condenser microphones were used to measure the pressure in the far field of the jet. The microphones were pre-amplified and powered by a NEXUS conditioning amplifier with high-pass filters set at 20 Hz. The microphones were mounted parallel to the jet and the origin is the centre of the jet nozzle exit. The distance between the origin and the closest microphone (observer polar angle $\theta = 90^o$, see Fig. 2(b)) is 2.13 m, or 53 jet nozzle diameters (D_j). The microphone sensitivities were obtained before and after the tests were performed. The calibration was carried using a B&K Type 4220 pistonphone calibrator.

2.3 Data acquisition and post-processing

All data was acquired using a 24-bit National Instruments dynamic signal acquisition system. An eight-channel NI PXI-4472 was used to acquire ambient chamber and pipe data, which were sampled at 1 kHz. Microphone measurements were sampled at 200 kHz. Test points were all acquired in 10-second samples.

The raw data was converted from TDMI format into Matlab .mat files. Pressure in Pascal was obtained by dividing the voltage raw data by each microphone's sensitivity derived from the calibration procedure and the gain set for each channel (31.6 V in this campaign). Sound pressure level (SPL) were achieved by dividing the Welch's power spectral density estimate of the pressure data divided by the reference pressure, $p_\mathrm{ref} = 20$ μPa. The SPL was then corrected for atmospheric attenuation effects and to a 1 meter lossless distance to the jet nozzle origin.

3. RESULTS

In this section, the main results of the experimental test are presented and discussed.

3.1 Summary of the results

All data was processed using the procedure briefly described in Section 2.3. The classic increase in SPL with core jet exit velocity was observed. Figure 3(a) shows the SPL for eight static jet speeds. The chamber background noise is also shown. At $M_\mathrm{j} = 0.2$ and 0.3, there is a spurious high frequency noise source around 40 kHz dominating the signal. Nonetheless, these frequencies are out of the range of interest (Strouhal number greater than 10, which is not important for the aircraft engine noise problem). In Fig. 3(b), the SPL of in-flight jets are shown. The flight velocity displayed is equals to $M_\mathrm{f} = 0.2$. Note that jet velocities below $M_j = 0.5$ are not displayed. As a general rule based on the data studied here, if the core jet velocity is not more than two times greater than the flight velocity, most of the far field spectrum is affected by the flight background noise. This is also in agreement with the relationship between the velocity ratio ($U_\mathrm{j}/U_\mathrm{f}$) and the area ratio ($D_\mathrm{j}^2/D_\mathrm{f}^2$). It is well-known that the pressure intensity in the far field will vary roughly with U^8 and D^2.

Figure 4(a) displays the SPL of an $M_\mathrm{j} = 0.8$ discharged at ambient media moving at different speeds. It is clear that increasing the flight flow velocity consistently reduces the noise produced by the core jet. This result is in agreement with large-scale open jet wind tunnels. Recently, it was also demonstrated that the turbulence intensity levels and the two-point coefficients within the turbulence source region also decrease with an increasing flight velocity (Proenca *et al.*, 2019). Therefore, acoustic and aerodynamic trends are in agreement.

Another important feature is the effect of the flight background noise at low frequencies. Note that, in Figure 4(a), at $M_\mathrm{f} = 0.3$ (light green curve), the jet SPL is contaminated up to around 2 kHz. To show this feature more clearly, Fig. 4(b) displays SPL for an $M_\mathrm{j} = 0.9$ core jet discharged in flight flow velocities $M_\mathrm{j} = 0.1$, 0.2 and 0.3. The flight background levels of the two slowest flight velocities (black and red curves) are considerably below the in-flight jet SPL. However, at $M_\mathrm{j} = 0.3$, some flight noise dominate at low frequency. The flight background sound pressure levels must be kept in mind when analysing data for the fastest flight velocities analysed in this work.

The other core jet and flight velocities presented similar results. Therefore, the key points to take from this sub-section are: 1) the pressure intensity at a given observer location decrease with increasing flight velocity, a trend that is in agreement with the flight effects on the turbulence levels in the jet (Proenca *et al.*, 2019); and 2) the flight background noise dominates the very low frequencies of the spectrum for exit velocities $M_\mathrm{f} > 0.5M_\mathrm{j}$.

In the next two sub-sections, the sound pressure level scaling with jet and flight velocities is surveyed.

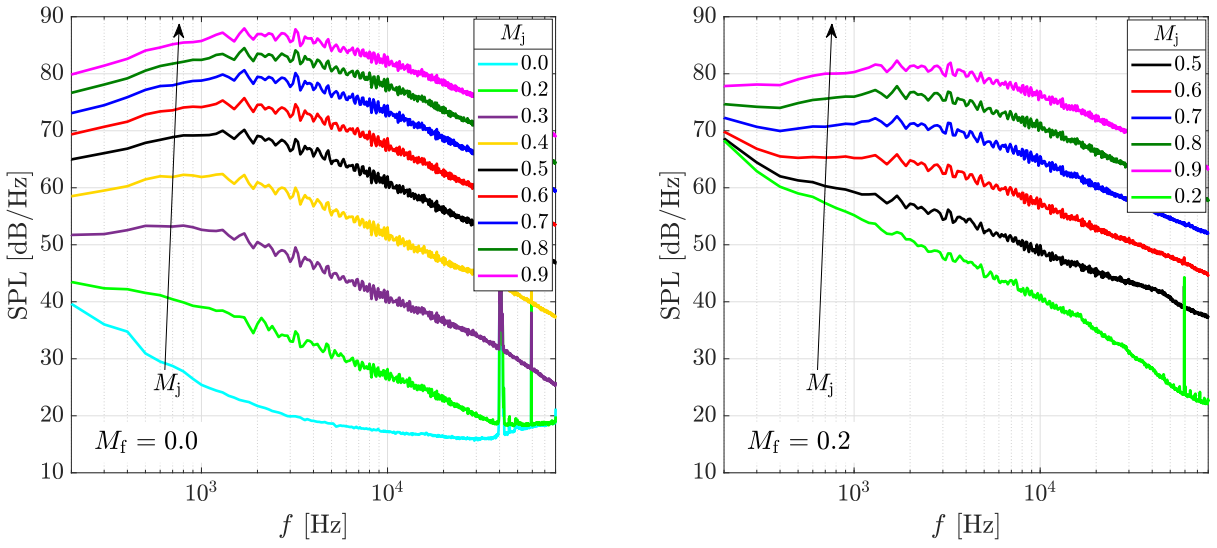

(a) $M_f = 0.0$ (b) $M_f = 0.2$

Figure 3. Sample sound pressure level results: (a) Background noise and static jet at set at eight jet nominal acoustic Mach numbers. (b) Flight background and $M_f = 0.2$ in-flight jets at five jet nominal acoustic Mach numbers

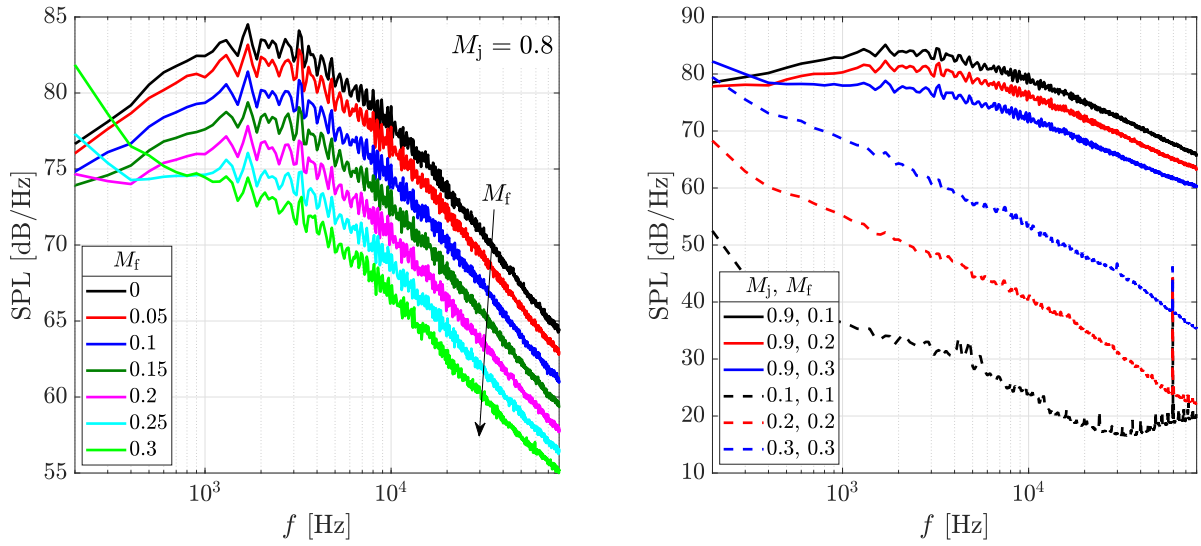

(a) (b)

Figure 4. SPL of in-flight jets. (a) Seven flight velocities, $M_j = 0.8$. (b) Three flight velocities, $M_j = 0.9$ and flight background noise

3.2 Far field SPL scaling with flight velocity

Using dimensional analysis, Lighthill suggested that the acoustic pressure field of static, subsonic jets scale with the jet exit velocity to the eighth power (Lighthill, 1952). This seminal paper was published before any experimental studies were available. Since then, experimental evidence has shown that the eighth power law works well for observer polar angles $\theta > 90^0$ (polar angles as defined in Fig. 2(b)). For lower polar angles, however, the exponent consistently increases from eight as the polar angle is decreased (see, for example data shown in Proenca (2018)).

The reason behind the variation of this exponent for different polar angles is not well-established. It is known that sound waves propagating towards the low polar angles are refracted, creating the so-called cone of silence in that region(Atvars *et al.*, 1965). Convection of the jet mixing noise source is considered by some authors, as the small-scale structures generating high frequency noise in the far field are transported by the mean flow (Tam *et al.*, 2008). Additionally, large coherent structures develop within the jet shear layer and instability wave theory is commonly used nowadays to model the jet noise source (Papamoschou, 2018). Whether the broadening of the static jet spectrum with observer

polar angle is due to two distinct noise sources (fine-scale and large-scale) or the growing instability effect still is an open question. Adding forward flight effects to this problem certainly does not simplify the analysis.

In this section, therefore, the far field spectrum of static and in-flight jets are discussed for an observer at $\theta = 90^o$ only. The changes with observer polar angle will be discussed in the next section. Figure 5 presents the far field scaling with jet and flight velocities. Each sub-plot show several core jet velocities for a fixed flight velocity. Note that flight background noise was not removed, so it shows clearly were the data suffers from background noise contamination. The frequency was normalised by the jet nozzle diameter and the velocity difference, $U_\mathrm{j} - U_\mathrm{f}$. The sound pressure level was corrected using the ratio $(U_\mathrm{j} - U_\mathrm{f})/U_\mathrm{ref}$. The reference velocity was derived from a reference Mach number, $M_\mathrm{j} = 0.8$ and depends on the ambient and flow conditions of each testpoint. This reference velocity scales all the different jet velocities displayed in each sub-graph. The velocity difference should scale the levels of the jets discharged at different flight velocities. As the power spectral density was used to calculate the SPL, the sound intensity in Figure 5 scales with U_j^7. This is due to the fact the Fourier transform of the pressure signal leads to units of pressure squared by frequency, or $\mathrm{Pa}^2\mathrm{s}$. Integrating the SPL for the frequencies of interests leads to the overall sound pressure level, which then scales with the classical U_j^8.

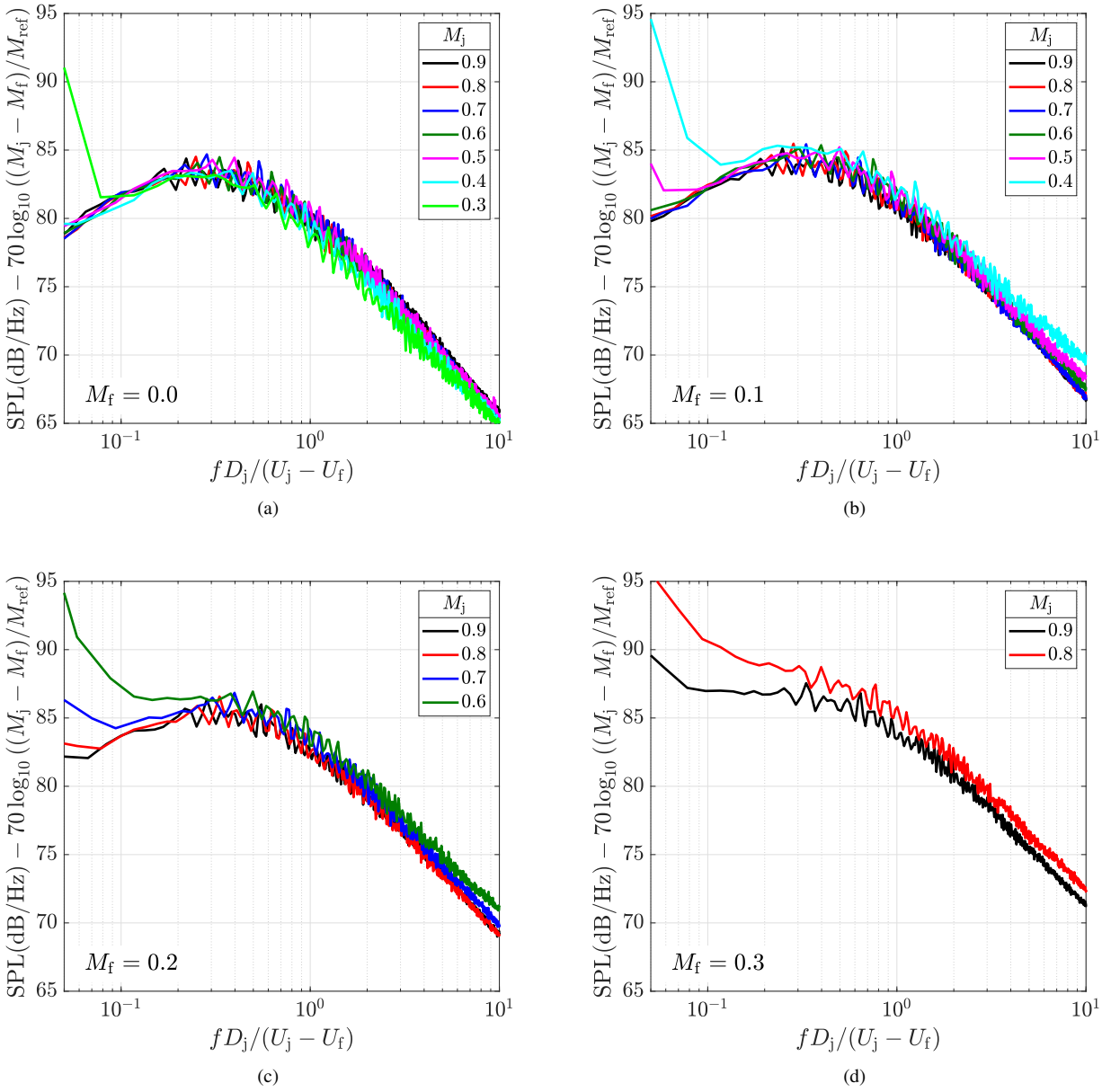

Figure 5. SPL scaling with core jet exit velocity. (a) $0.3 \leq M_\mathrm{j} \leq 0.9$, $M_\mathrm{f} = 0.0$. (b) $0.4 \leq M_\mathrm{j} \leq 0.9$, $M_\mathrm{f} = 0.1$. (c) $0.6 \leq M_\mathrm{j} \leq 0.9$, $M_\mathrm{f} = 0.2$. (d) $0.8 \leq M_\mathrm{j} \leq 0.9$, $M_\mathrm{f} = 0.3$

In summary, scaling of the SPL shows that the velocity difference to the seventh power is the correct parameter to

collapse both the far field noise levels and the spectra shape. A clear exception to the rule is the low frequency content of the lowest jet velocities in all sub-graphs of Figure 5. This is due to 1) the bandwidth used in the averaging of the pressure signal blocks (bandwidth= 100 Hz) and 2) the flight background noise in figures 5(b) to 5(d). As mentioned before, the latter was shown on purpose to highlight the scaling does not work in these frequencies due to far field noise contamination. A lower bandwidth increases the resolution at the spectra at low frequencies, but also makes the graphs unreadable in the high frequencies. Nonetheless, it is clear that the parameters used provided a correct scaling with the velocity difference.

Observing the SPL peak of each sub-figure, ignoring the DC component value, the peak increases with flight velocity. This essentially demonstrates the problem seen in other experimental datasets: the far field noise of in-flight jets scale with a lower exponent when fixing the jet Mach number at the nozzle exit and varying the flight velocity. This is discussed further in the next section, where the overall sound pressure level (OASPL) and the other observer polar angles are investigated.

3.3 Far field OASPL scaling with flight velocity

The overal sound pressure level was obtained by integrating the sound pressure level from Strouhal numbers based on the velocity difference in the range $0.1 \leq fD_\mathrm{j}/\left(U_\mathrm{j} - U_\mathrm{f}\right) \leq 10$. Figure 6 shows the OASPL for several static jets at the polar angles studied. Figure 6(a) uses the eighth power of the velocity difference to scale the data, whilst Fig. 6(b) shows the scaling with the ninth power. As discussed previously, the eighth power collapses the pressure intensity for observers located at $\theta \geq 90^o$. The difference of 5 dB between the $M_\mathrm{j} = 0.3$ and $M_\mathrm{j} = 0.9$ jets at $\theta = 40^o$ is clearly not due to any uncertainties associated with the experiment, but rather an effect which is not accounted for in the scaling derived from dimensional analysis. Figure 6(b) demonstrates that a power of nine is more appropriate for that particular polar angle and intermediate exponents collapse the data for angles between $\theta = 40^o$ and $\theta = 90^o$.

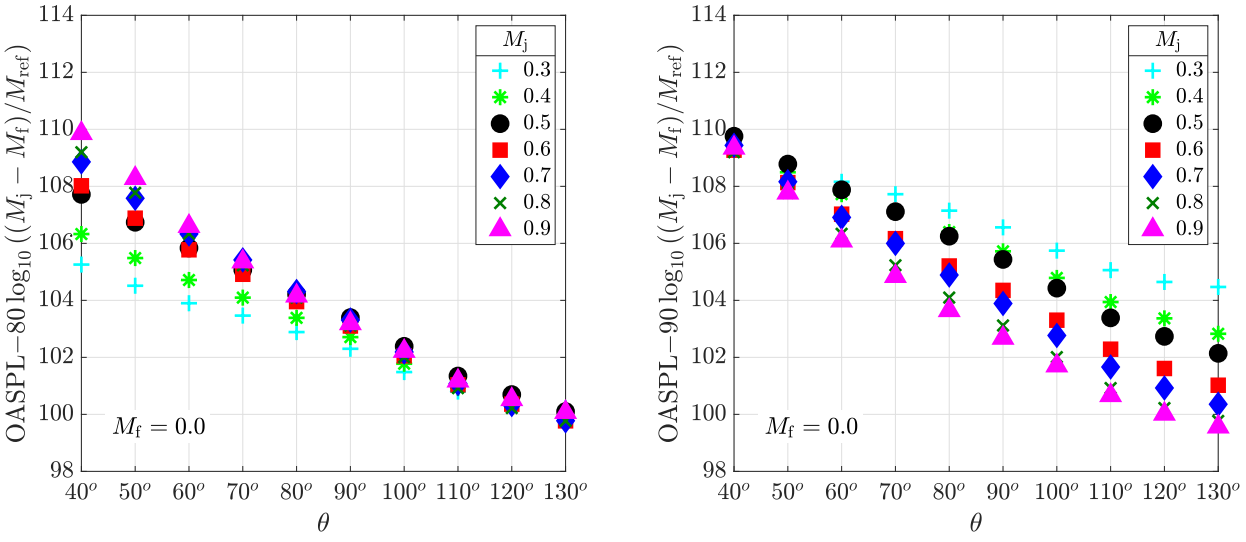

(a) (b)

Figure 6. Scaling of the far field OASPL with jet exit velocity. (a) Scaling with U^8_rel. (b) Scaling with U^9_rel. Note that the data presented here is for a static jet ($M_\mathrm{f} = 0$)

Figure 7 illustrates the OASPL of in-flight jets at different observer locations. Two flight velocities are used, $M_\mathrm{f} = 0.05$ in Fig. 7(a) and $M_\mathrm{f} = 0.2$ in Fig. 7(b). The acoustic pressure field of the jet velocities shown in each graph are free of flight background contamination. It is interesting to note the consistent trend as the flight velocity is increased. At relatively high flight velocities, there is a good agreement in low polar angles with the exponent that collapse the far field in the forward arc of static jets. A power slightly lower than eight is seen to collapse the data at high polar angles.

A direct comparison between figures 6(a) and 7(b) shows that there is a shift in the OASPL directivity of around 20^o from the static jet to the $M_\mathrm{f} = 0.2$ in-flight jet. As the far field data has been corrected to a 1 meter lossless distance from the jet origin, this leads to a shift in location of 0.35 m, or $8.75D_\mathrm{j}$. This is partly explained by the stretching of the jet discharged in a forward flight flow. The potential core of the core jet nozzle studied in this work elongates from $4.65D_\mathrm{j}$ in the static jet to $7.85D_\mathrm{j}$ in the $M_\mathrm{f} = 0.2$ in-flight jet. Another effect is the different eddy convection velocity of these two configurations. In the region of high turbulent kinetic energy, the eddy convection velocity are about $0.55U_\mathrm{j}$ and $0.65U_\mathrm{j}$ for the static and in-flight cases, respectively (Proenca *et al.*, 2019). The increase in the eddy convection velocity,

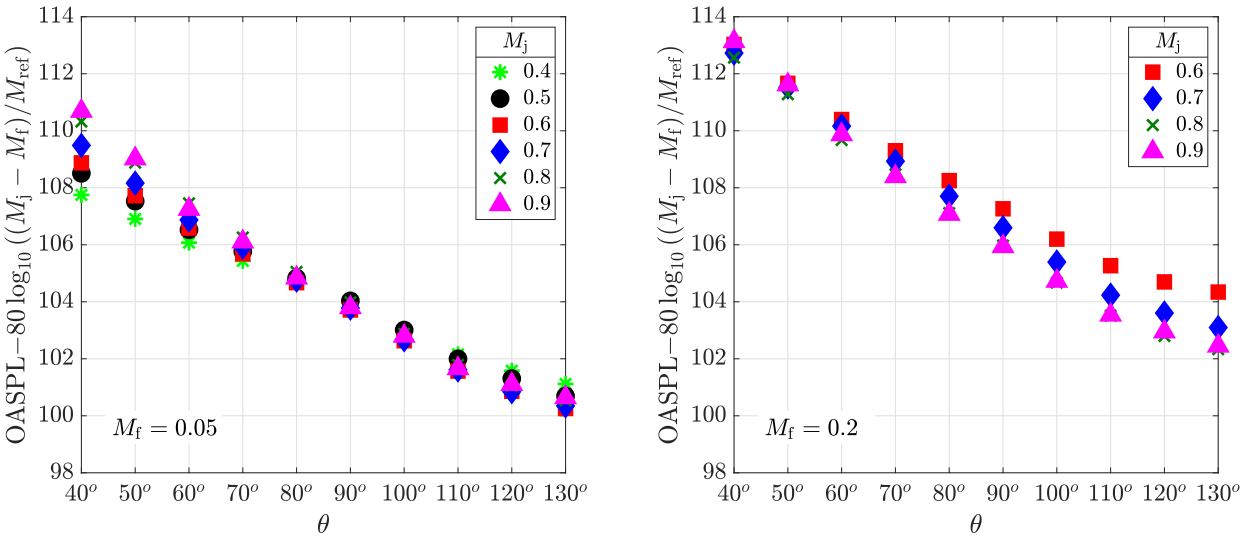

(a) (b)

Figure 7. Scaling of the far field OASPL with the eighth power of the velocity difference. (a) Flight Mach number $M_\mathrm{f} = 0.05$. (b) Flight Mach number $M_\mathrm{f} = 0.2$

therefore, impacts on the far field directivity by directing more energy towards the rear arc, which is consistent with the results shown in figures 6 and 7.

Based on the results discussed in this section and presented in previous research for large-scale facilities, it is clear that Lighthill's dimensional analysis fails to scale the pressure intensity for a jet discharged in ambient media of different velocities. A result of this procedure is shown in Figure 8(a). As the energy shift towards lower polar angles, the OASPL at a given observer location is relatively higher at increasing flight velocities. This lead researchers to define empirical scaling of the forward flight effects on the jet far field. This empirical exponent is usually around five for most angles and a lower power is more appropriate at the forward arc (Bryce, 1981; Viswanathan, 2018). An example of the scaling of the OASPL with $(U_\mathrm{j} - U_\mathrm{f})^5$ is shown in Fig. 8(b).

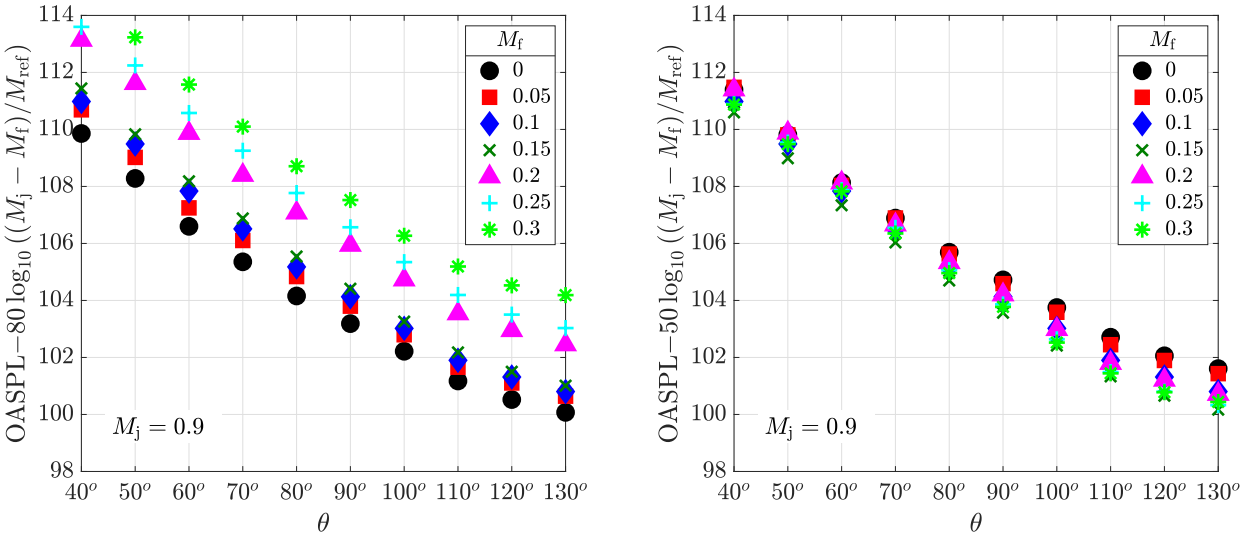

(a) (b)

Figure 8. Scaling of the far field OASPL with the velocity difference. (a) Scaling with U_rel^8. (b) Scaling with U_rel^5. Jet nominal Mach number $M_\mathrm{j} = 0.9$ for all curves

Taking into account the apparent shift of the OAPSL with flight velocity, it is possible to collapse the pressure intensity using the eighth power of the velocity difference and a convection factor for the observer polar angles. It was observed that the 0.05 Mach number increments used in the test data would shift the OASPL levels around 5^o toward the rear arc.

Thus, a simple empirical correction of $\theta - 100M_\mathrm{f}$, where θ is measured in degrees, collapse the OASPL curves. Figure 9 displays the results of this procedure.

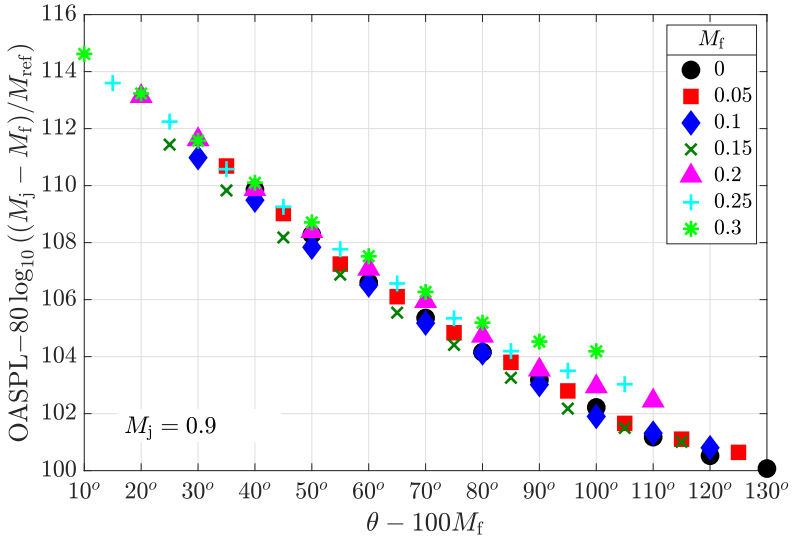

Figure 9. OASPL scaling with flight velocity at several polar angles based on the Lighthill's coefficient. Note the polar angle is corrected for the flight velocity

The collapse of OASPL from several different flight velocities using the velocity difference and the shift in polar angle is remarkable. The trend seems to be valid even for very low polar angles, where the in-flight jet data was extrapolated. This is in good agreement with the hypothesis discussed above, namely the increase in eddy convection velocity with increasing flight velocity and the stretching of the jet. This is a new explanation to the scaling of forward flight effects and the reason the dimensional analysis fails to provide the correct power for the flight effects.

4. CONCLUSIONS

In this paper, the pressure far field of in-flight jets has been investigated. Experimental results shown that a small-scale open jet wind tunnel produces results that are comparable to data from large-scale facilities published previously. Thus, no significant Reynolds number effects are present. This is important to establish these low cost, high fidelity university rigs to the study of forward effects on jet noise and jet installation noise.

The far field of static jets are shown to scale as suggested by dimensional analysis of the problem. The variation of the power to which the SPL varies with velocity at different observer angles still lacks a satisfactory explanation. Nonetheless, results presented here are consistent and provide confidence to the novel in-flight jet data analysed.

The systematic increase in both core jet velocity and flight velocity presented in the paper has allowed a careful study of the scaling of in-flight jets to be performed. The classical analysis presented in the literature of fixing a jet exit velocity and varying the flight velocity show that the pressure intensity in the far field is function of the velocity difference raised to a power lower than 8. The power law varies slightly with polar angle and an exponent around 5 collapses most of the locations studied. This is similar to results obtained in other facilities.

The main contributions of this work consist of 1) demonstrating that a power of 8 of the velocity difference is the correct parameter when the flight velocity is fixed and several jet velocities are analysed; and 2) that a correction for the polar angle, as a function of the flight velocity, collapses all the data studied in the paper. The evidence provided for the first argument suggests that the dimensional analysis of a static jet is still valid for in-flight jets. Aerodynamic results shared in another paper (Proenca *et al.*, 2019) are now complemented by the second claim mentioned above. Combining the increase in convection velocity, jet stretching and the polar angle correction shown in Fig. 9, experimental evidence for the scaling of the far field of in-flight jets with both jet and flight velocities have been obtained. These findings will provide feedback into the prediction methodologies for jet mixing noise and jet-flap installation noise.

5. ACKNOWLEDGEMENTS

The authors would like to acknowledge the continuing financial support provided by Rolls-Royce plc through the Rolls-Royce University Technology Centre for Gas Turbine Noise at the University of Southampton's Institute of Sound and Vibration Research.

6. REFERENCES

Atvars, J., Schubert, L.K. and Ribner, H.S., 1965. "Refraction of sound from a point source placed in an air jet". *The Journal of the Acoustical Society of America*, Vol. 37, No. 1, pp. 168–170. doi:https://doi.org/10.1121/1.1909297.

Bryce, W., 1981. "The prediction of static-to-flight changes in jet noise". American Institute of Aeronautics and Astronautics, number 0 in Aeroacoustics Conferences. doi:10.2514/6.1984-2358. URL https://doi.org/10.2514/6.1984-2358.

Camussi, R., 2013. *Noise Sources in Turbulent Shear Flows: Fundamentals and Applications*. Springer-Verlag Wilen, CISM, Udine. ISBN 978-3-7091-1458-2.

Cocking, B. and Bryce, W., 1975. "Subsonic jet noise in flight based on some recent wind-tunnel tests". American Institute of Aeronautics and Astronautics, number 0 in Aeroacoustics Conferences. doi:10.2514/6.1975-462. URL https://doi.org/10.2514/6.1975-462.

Drevet, P., Duponchel, J. and Jacques, J., 1977. "The effect of flight on jet noise as observed on the bertin aÃl'rotrain". *Journal of Sound and Vibration*, Vol. 54, No. 2, pp. 173 – 201. ISSN 0022-460X. doi:https://doi.org/10.1016/0022-460X(77)90022-0. URL http://www.sciencedirect.com/science/article/pii/0022460X77900220.

Larson, R.S., MeColgan, C.J. and Packman, A.B., 1978. "Jet noise source modification due to forward flight". *AIAA Journal*, Vol. 16, No. 3, pp. 225–232. doi:10.2514/3.60881. URL https://doi.org/10.2514/3.60881.

Lighthill, M.J., 1952. "On sound generated aerodynamically. I. General theory". *Proceedings of the Royal Society of London A: Mathematical, Physical and Engineering Sciences*, Vol. 211, No. 1107, pp. 564–587. ISSN 0080-4630. doi:https://doi.org/10.1098/rspa.1952.0060.

Papamoschou, D., 2018. "Wavepacket modeling of the jet noise source". *International Journal of Aeroacoustics*, Vol. 17, No. 1-2, pp. 52–69. doi:10.1177/1475472X17743653. URL https://doi.org/10.1177/1475472X17743653.

Plumblee, Jr., H.E., 1976. "Effects of forward velocity on turbulent jet mixing noise". Technical report.

Proenca, A.R., Lawrence, J.L.T. and Self, R.H., 2019. *Experimental Investigation into the Turbulence Flow Field of In-Flight Jets*. doi:10.2514/6.2019-2545. URL https://arc.aiaa.org/doi/abs/10.2514/6.2019-2545.

Proenca, A.R., 2018. *Aeroacoustics of isolated and installed jets under static and in-flight conditions*. Ph.D. thesis, University of Southampton. URL https://eprints.soton.ac.uk/426880/.

Tam, C.K.W., Viswanathan, K., Ahuja, K.K. and Panda, J., 2008. "The sources of jet noise: experimental evidence". *Journal of Fluid Mechanics*, Vol. 615, pp. 253–292. doi:10.1017/S0022112008003704.

Tanna, H. and Morris, P., 1977. "In-flight simulation experiments on turbulent jet mixing noise". *Journal of Sound and Vibration*, Vol. 53, No. 3, pp. 389 – 405. ISSN 0022-460X. doi:https://doi.org/10.1016/0022-460X(77)90422-9. URL http://www.sciencedirect.com/science/article/pii/0022460X77904229.

Viswanathan, K., 2018. "Progress in prediction of jet noise and quantification of aircraft/engine noise components". *International Journal of Aeroacoustics*, Vol. 17, No. 4-5, pp. 339–379. doi:10.1177/1475472X18778279. URL https://doi.org/10.1177/1475472X18778279.

7. RESPONSIBILITY NOTICE

The authors are the only responsible for the printed material included in this paper.